Nuclear Instruments and Methods in Physics Research A 371 (1996) 295–299

NUCLEAR INSTRUMENTS & METHODS IN PHYSICS RESEARCH
Section A

ELSEVIER

# The RICH detector for HERA-B

P. Križan[a,b], S. Korpar[c], M. Starič[a,*], A. Stanovnik[a,d], M. Çindro[a], G. Močnik[a], D. Škrk[a], M. Zavrtanik[a], A. Bulla[e], E. Michel[e], P. Weyers[e], W. Schmidt-Parzefall[e], T. Hamacher[f], R. Schwitters[f]

[a] *J. Stefan Institute, University of Ljubljana, Ljubljana, Slovenia*
[b] *Department of Physics, University of Ljubljana, Ljubljana, Slovenia*
[c] *Technical Faculty, University of Maribor, Maribor, Slovenia*
[d] *Faculty of Electrical Engineering and Computer Sciences, University of Ljubljana, Ljubljana, Slovenia*
[e] *DESY, Hamburg, Germany*
[f] *University of Texas, Austin, TX, USA*

**Abstract**

The expected performance of the Ring Imaging Cherenkov (RICH) detector to be used in the HERA-B experiment is discussed.

## 1. Introduction

The main purpose of the HERA-B experiment, at the HERA collider in Hamburg, is to study CP violation in the decays $B^0$ (or $\overline{B^0}$) $\rightarrow J/\Psi\ K_s^0 \rightarrow l^+l^-\ \pi^+\pi^-$ [1]. The experiment will use thin-ribbon targets in the halo of the 820 GeV proton beam, so it should not disturb the experiments measuring e–p collisions. From the estimated ratio of cross sections, it follows that one desired $B^0$ decay occurs per $10^{11}$ proton–nucleus interactions. An interaction rate of about 40 MHz is thus required in order to detect a few thousand of the $B^0$ decays per year. As the time interval between successive proton bunches is 96 ns, this interaction rate is equivalent to an average of 4 interactions per bunch crossing. The HERA-B experiment is designed to search for the B decays among the 200 odd particles produced by each proton bunch (Fig. 1). It is the specific task of the RICH to tag the $B^0$ (or $\overline{B^0}$) meson by identifying the charged kaon into which the associated B meson decayed. The RICH counter should therefore be capable of separating kaons from pions over most of the kaon momentum range and of resolving between particles belonging to successive bunch crossings. This task must be performed reliably over long periods of time in the hostile environment of about 2 GHz of charged particles.

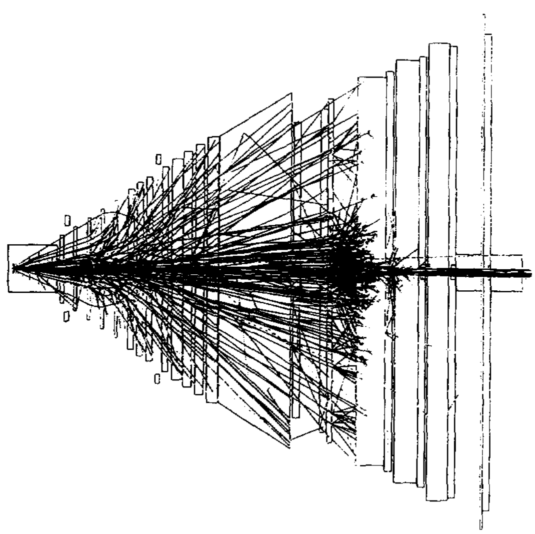

Fig. 1. Simulated tracks due to one bunch crossing in the HERA-B experiment.

* Corresponding author.

## 2. Expected performance of the RICH

Tagging of the $B^0$ (or $\overline{B^0}$) meson is achieved by identifying the charged kaon into which the associated B meson decayed. The momentum distribution of charged kaons, resulting from decays of the associated B mesons, which are in turn produced by 820 GeV protons incident on a fixed target, is shown in Fig. 2. Identifying the charged kaon essentially means separating it from the pion of the same momentum. The momentum of the particles is accurately measured in other components of the HERA-B detector, so separation in mass is equivalent to separation

0168-9002/96/$15.00 © 1996 Elsevier Science B.V. All rights reserved
*SSDI* 0168-9002(95)01176-5

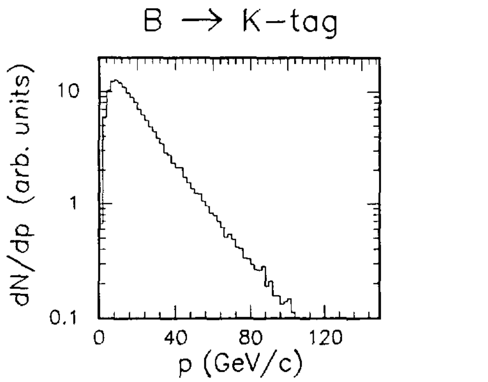


Fig. 2. The momentum distribution of charged kaons produced in decays of B mesons associated to the production of the $B^0$ (or $\overline{B^0}$) meson by proton–nucleus interactions at 820 GeV.

in velocity. At high momenta ($pc \gg m_0c^2$) the difference in velocity of the two particles however, is proportional to the inverse square of the momentum, so the separation becomes increasingly more difficult. For example the π–K velocity difference is $\Delta\beta = 1.12 \times 10^{-3}$ at 10 GeV/$c$ and it reduces to $4.5 \times 10^{-5}$ at 50 GeV/$c$.

The Ring Imaging Cherenkov detector is expected to achieve the required π–K separation by accurately measuring the Cherenkov angle in a gas radiator. Perfluorobutane gas ($C_4F_{10}$) has been chosen for its very good UV transparency and for its relatively low dispersion ($n = 1.00153$, $dn/dE = 5.3 \times 10^{-5}\ eV^{-1}$) [2]. In this gas, the Cherenkov threshold for pions is at 2.6 GeV/$c$ and for kaons it is at 9.0 GeV/$c$. For $\beta = 1$ particles, the Cherenkov angle is 55.6 mrad, while the π–K difference in angle is about 28 mrad at 10 GeV/$c$ and falls to 0.8 mrad at 50 GeV/$c$.

Contributions to the angular spread of Cherenkov photons, emitted by a single particle, come from chromatic aberration and multiple Coulomb scattering of the charged particle in the radiator, from spherical aberration, misalignment and other imperfections of the mirrors and from the position resolution of the photon detectors. Over the sensitive range of the photon detectors ($\Delta E \sim 1.3$ eV FWHM, see Fig. 7 below), chromatic aberration in $C_4F_{10}$ ($\Delta E \times dn/dE \sim \Delta n \sim 6.9 \times 10^{-5}$) introduces a spread $\Delta\theta_{ch} \sim \Delta n/\theta_{ch}$ in the individual photon angle, which at higher momenta equals approximately 1.2 mrad FWHM. The standard deviation $\sigma_{\Delta_n}$ obtained by proper integration is about 0.4 mrad.

A schematic drawing of the RICH inside the HERA-B detector is shown in Fig. 3. The 2.7 m along the beam pipe, available for the RICH, will be filled with $C_4F_{10}$ gas at normal temperature and pressure. The radiation length of $C_4F_{10}$ and the average multiple Coulomb scattering angle of charged particles in 2.7 m of $C_4F_{10}$ have been calculated according to the formulae given in the literature [3]. A radiation length of 35 m has been obtained, which leads to $\sigma_{MCS} = 0.4$ mrad at 10 GeV/$c$ and $\sigma_{MCS} = 0.1$ mrad at 50 GeV/$c$.

The RICH detector is composed of two arms; one above and the other below the beam pipe. Each arm consists of a spherical mirror, a planar mirror and of photon detector modules in the focal surface (Figs. 3 and 4). The spherical mirrors are tilted in order to reflect the Cherenkov photons onto the corresponding planar mirror, after which the photons converge to a ring in the focal surface. With such an arrangement, the focal surface and thus the photon

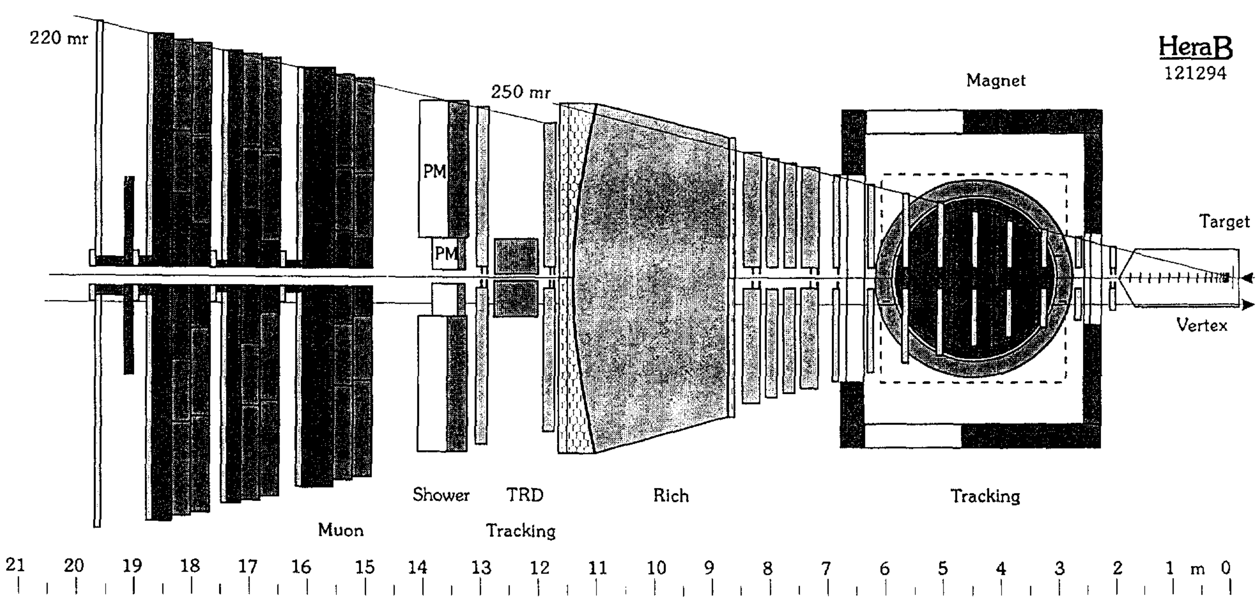


Fig. 3. Schematic drawing of the HERA-B detector.

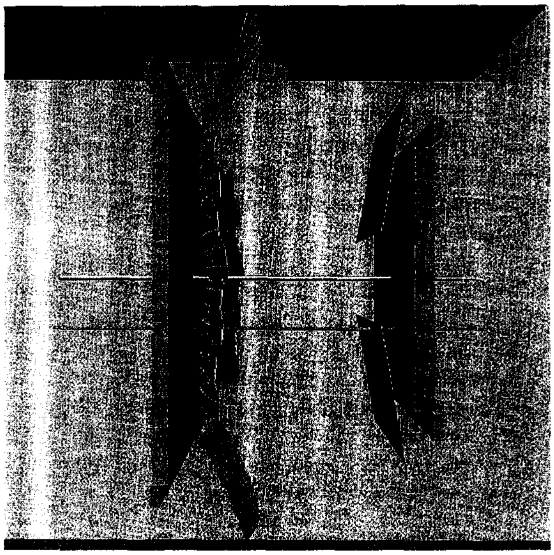

Fig. 4. A computer generated view of the RICH. The spherical mirrors and the photon detectors are composed of hexagonal and rectangular modules respectively. Besides the proton beam pipe, also the electron beam pipe must pass through the apparatus.

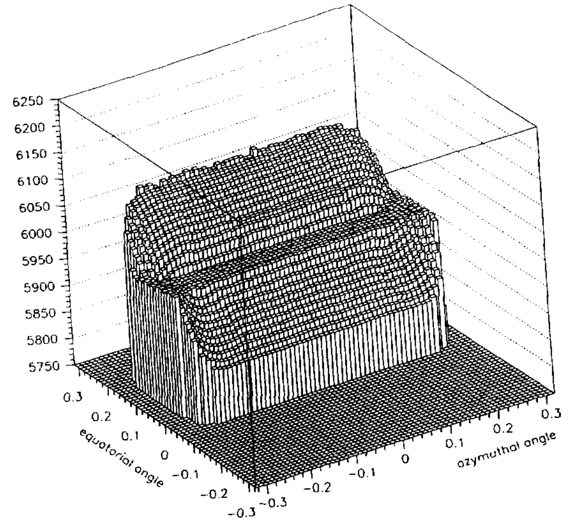


Fig. 5. The calculated focal surface given in spherical coordinates. The origin of the coordinate system is in the center of curvature of the tilted spherical mirror (9° tilt). The $x$-axis is parallel to the beam axis, the $z$-axis is vertical and the $y$-axis is horizontal. The additional reflection on the plane mirror (see Fig. 4) is not taken into account.

detectors are removed from the main charged particle flux, which would cause an unacceptable background. The drawback of such a solution however, is an increase in spherical aberration as a result of tilting the spherical mirrors. A focal surface, defined as the surface of minimum average spread of the Cherenkov photon hits, has been calculated [4]. This surface is shown in Fig. 5 for charged particles with $\beta = 1$, radiating in $C_4F_{10}$ ($\theta_{ch}$ = 55.6 mrad) and incident onto a spherical mirror of 11.5 m radius, which is tilted for 9°. A substantial displacement of the focal surface from the $f = r/2$ approximation is observed. By placing the photon detectors in this focal surface, one should reduce the error due to spherical aberration. Monte Carlo simulation and reconstruction for the cases that the photon detectors are located in the true focal surface, at $r/2$ or at $1.03 \times r/2$ result in single-photon standard deviations of 0.16, 0.29 and 0.17 mrad respectively (Fig. 6). A very good approximation to the focal surface of Fig. 5 is a spherical surface with a displaced center of curvature. In the coordinate system of Fig. 5 this would be represented by a plane, best fitted to the true focal surface. Besides compensating for spherical

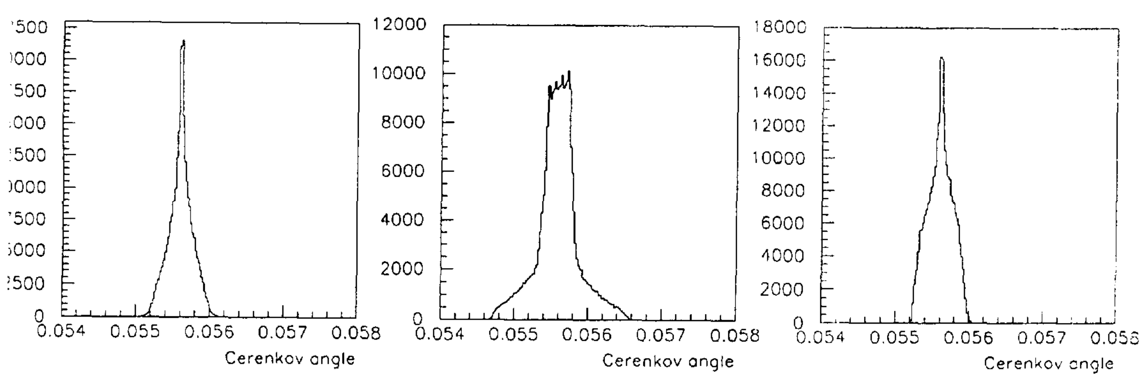


Fig. 6. Spherical aberration depending on the position of photon detectors. The distribution of the Cherenkov angle, obtained by simulation and reconstruction of single photons emitted by $\beta = 1$ particles is shown for the following cases: the photon detectors are in the true focal surface of Fig. 5 (left), the photon detectors are at the position of the $f = r/2$ approximation (center), the photon detectors are placed at $1.03 \times r/2$ (right).

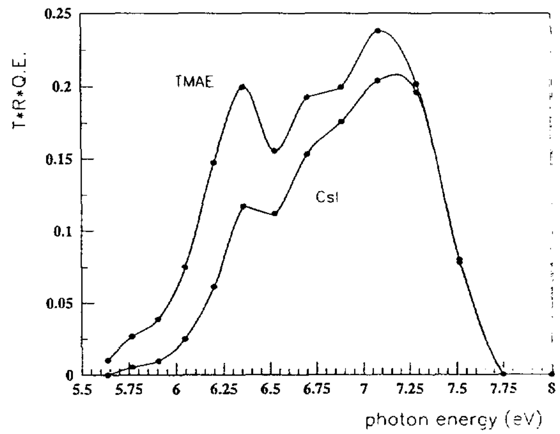


Fig. 7. The dependence on photon energy of the product of gas and window transmission, mirror reflectivity and quantum efficiency for the two candidate photon detectors.

aberration such a position of the photon detectors results in increased efficiency for the TMAE detectors. The efficiency increases because the average incidence angle is smaller and there is less photon absorption in the walls dividing the unit cells [5]. Contributions such as misalignment and other optical imperfections of the mirrors are neglected in the present estimates.

The position resolution of the photon detectors also contributes to the accuracy with which the Cherenkov angle is determined. For the two options that are being considered for photon detection, the pixel size is 8 mm × 8 mm for the TMAE detectors [5] and 7.5 mm × 7.5 mm for the CsI detectors [6]. A uniform distribution of hits within the pixel leads to a standard deviation of $\sigma_x^{\mathrm{det}} \sim \Delta x/\sqrt{12}$. The corresponding uncertainty in Cherenkov angle is $\sigma_{\mathrm{det}} = \sigma_x^{\mathrm{det}}/f$, where $f = 5.75$ m is the focal length of the spherical mirror. One thus obtains a standard deviation of about $\sigma_{\mathrm{det}} = 0.4$ mrad for both types of detectors.

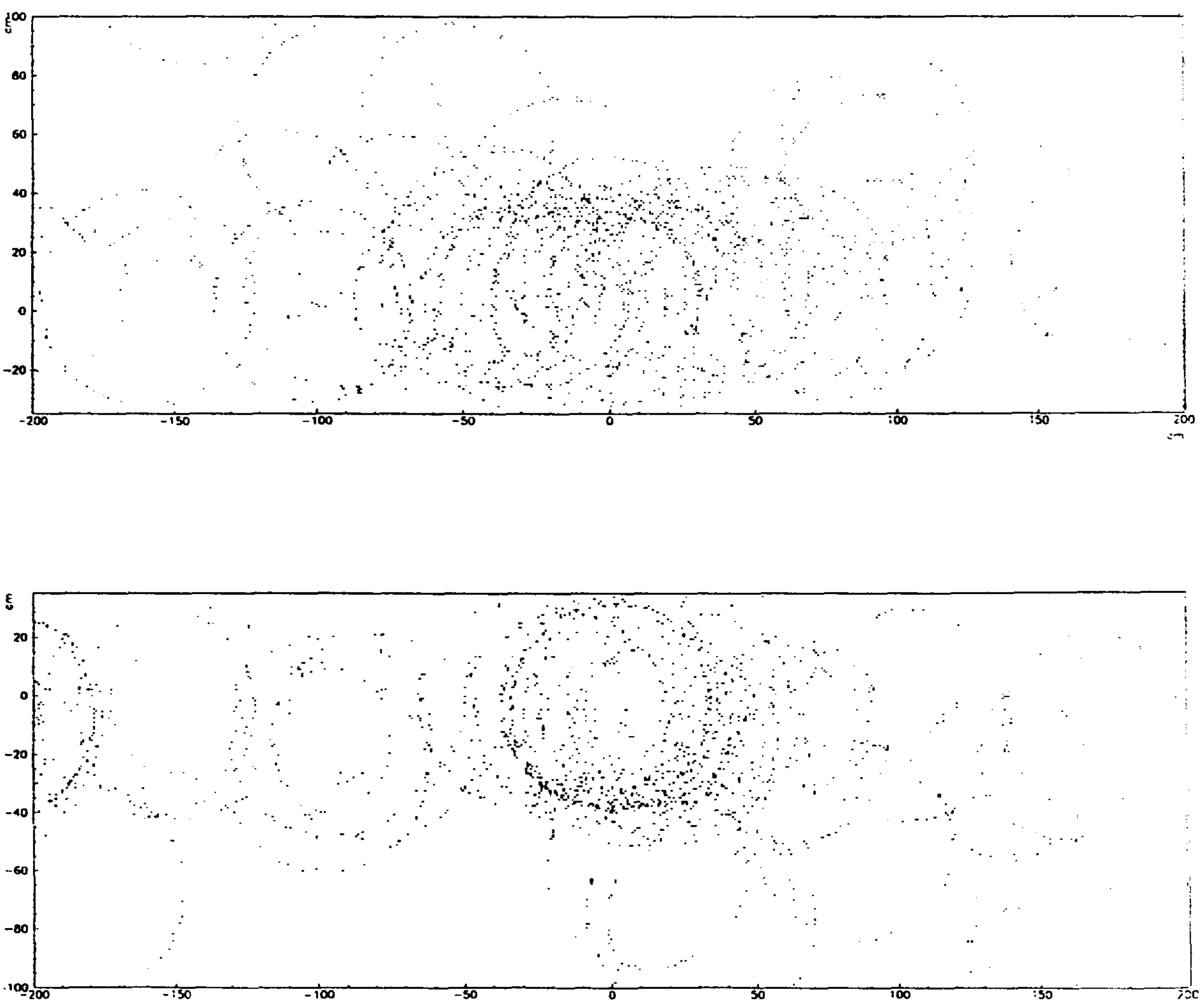


Fig. 8. A computer simulated pattern of Cherenkov photon hits on the photon detector due to one bunch crossing.

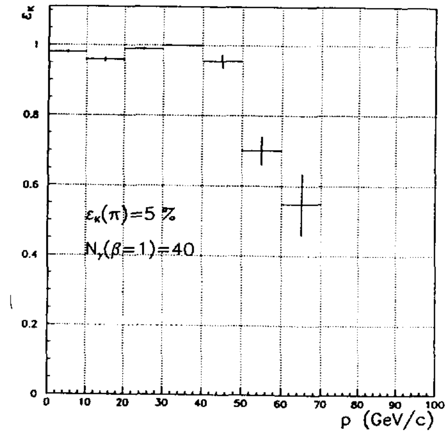


Fig. 9. The momentum dependent efficiency for resolving a kaon in the background of other particles in the event. It was assumed that on average 40 photons are detected per $\beta = 1$ track and that a single photon determines the particle velocity with $\sigma_\beta = 3.3 \times 10^{-5}$.

By summing the squares of all the contributions, one obtains an estimate for the standard deviation of the distribution of Cherenkov angle determined from a single photon hit as $\sigma(1\ \mathrm{hit}) \sim 0.6$ mrad at 50 GeV/$c$. However, more than one Cherenkov photon will be detected per charged particle track, with the result that their average angle is determined to a better accuracy. The standard deviation of this average angle is proportional to the inverse square root of the number of detected photons per ring. The number of detected photons depends on a number of factors: the velocity of the particle, the refractive index and thickness of the radiator, the reflectivity of the mirror, absorption in the gas and in the windows, on the quantum efficiency of the photocathode and on the photoelectron detection efficiency. The product of some of these factors is shown in Fig. 7 for two options of photon detection: TMAE [5] or CsI [6]. The expected number of detected photons is given by the expression $N_{\mathrm{ph}} = N_0 L \sin^2\theta_{\mathrm{ch}}$, where $N_0$ has been calculated to be 42 cm$^{-1}$ for the TMAE detector and 48 cm$^{-1}$ for the CsI detector. For a $\beta = 1$ particle, one expects about 35 detected photons in the TMAE detector and about 40 in the CsI photon detector. With 40 detected photons, the proposed Ring Imaging Cherenkov detector should achieve a $3\sigma$ $\pi$–K separation up to about 80 GeV/$c$.

However, the estimates quoted above would be valid only for the case of isolated single particles with no background. A large number of simultaneous particles, generated by one proton bunch crossing, radiate Cherenkov photons giving rise to a hit pattern as shown in Fig. 8. Simulation and reconstruction of such events shows, that, in the case that every charged particle radiates 40 Cherenkov photons, each of which leads to a velocity determination with $\sigma_\beta = 3.3 \times 10^{-5}$ and allowing 5% of pion fake probability, one obtains a kaon detection efficiency as shown in Fig. 9. It is obvious that the influence of background on the kaon detection efficiency is quite important.

## 3. Conclusions

From the discussion above, it may be observed, that the two major contributions to the spread in Cherenkov angle of the photons radiated by a single particle, are due to chromatic dispersion in the radiator (~0.4 mrad) and to the position resolution of the photon detectors (~0.4 mrad). The contribution of multiple Coulomb scattering decreases with increasing momentum and is negligible at 50 GeV/$c$. Spherical aberration of the tilted mirror produces a substantial displacement of the focal surface. However, this error may be compensated by placing the photon detectors in the calculated position of the focal surface. Therefore, the overall standard deviation of the Cherenkov angle, that would be obtained from a single photon and the given charged particle track direction (~0.6 mrad), is expected to be less than the $\pi$–K difference in Cherenkov angle at 50 GeV/$c$ (~0.8 mrad).

From the design parameters of the RICH, one estimates that about 40 Cherenkov photons could be detected per $\beta = 1$ charged particle, which allows a $3\sigma$ $\pi$–K separation up to approximately 80 GeV/$c$. However, a large background, in which the kaon must be found, is generated by Cherenkov radiation of the many other charged particles created in the same bunch crossing. Such a background reduces the momentum up to which the kaons and pions are separated with high efficiency. Nevertheless, the design parameters of the HERA-B RICH are such that a sufficient $\pi$–K separation is expected over most of the kaon momentum range.

## References

[1] P. Križan, R. Mankel, D. Ressing, S. Shuvalov and M. Spahn, Nucl. Instr. and Meth. A 351 (1994) 111.

[2] G. Lenzen, E. Schyns. J. Thadome and J. Werner, Nucl. Instr. and Meth. A 343 (1994) 268.

[3] Particle Data Group, Review of Particle Properties, Phys. Rev. D 50 (1994) 1173.

[4] P. Križan and M. Starič, Institute Jožef Stefan report IJS-DP-7053 (1994).

[5] T. Hamacher et al., these Proceedings (1995 Int. Workshop on Ring Imaging Cherenkov Detectors, Uppsala, Sweden) Nucl. Instr. and Meth. A 371 (1996) 289.

[6] P. Križan et al., ibid., p. 151.